

# The $\mu^+/\mu^-$ Ratio at the Depth of 3000 m.w.e.

N. Yu. Agafonova\*, V.V. Boyarkin\*, W. Fulgione<sup>†</sup>, A.S. Malgin\*, M. Selvi<sup>‡</sup>,  
O.G. Ryazhskaya\* on behalf of the LVD Collaboration

\*Institute for Nuclear Research of Russian Academy of Science

<sup>†</sup>Institute of Physics of Interplanetary Space, INAF, Torino

<sup>‡</sup>University of Bologna and INFN-Bologna, Italy

**Abstract.** The value of  $\mu^+/\mu^-$  -ratio for atmospheric muons has been measured with the LVD detector, at the INFN Gran Sasso National Laboratory, Italy (minimal depth is 3000 m.w.e.). To reach this depth muons should have an energy at the sea level higher than 1.3 TeV. The muon charge is determined studying the decay of stopping positive muons in the LVD iron structure and the decay of stopping positive and negative muons in scintillator. We obtain a ratio  $R = 1.26 \pm 0.11 \pm 0.04$

**Keywords:** atmospheric muons, underground experiment, charge composition

## I. INTRODUCTION

The charge ratio of cosmic ray muons has been studied since the muon discovery. The muon flux charge ratio was used for obtaining charge of primary cosmic rays (p.c.r.) because the ratio  $k = \mu^+/\mu^-$  for the muon energy  $E_\mu \geq 5$  GeV depends on p.c.r. charge ratio and characteristics of interactions of p.c.r. particles with air nuclei (differential cross-section of  $\pi^-$ - and K-mesons generation, total cross-section).

The charge composition of near-vertical muon flux is of particular interest because near-vertical muons dominate in the total flux. The available data obtained in  $\sim 20$  experiments at sea level up to  $P_\mu \sim 100$  GeV/c are in a good agreement with the standard concept about p.c.r. spectrum and  $pA$ - and  $AA$ - interactions in the corresponding range of p.c.r. energies below 0.6 TeV. The value of  $k$  may be considered as constant with the mean value of  $\bar{k}_\mu = 1.26$  with the error of about 2%.

For the energy higher than 100 GeV the number of studies is sufficiently smaller and the errors of  $\bar{k}_\mu$  are larger than 10% (except L3+C experimental result [1] having the errors less than 3% until  $P_\mu \sim 250$  GeV/c) what leads to the scatter of  $k$  from 0.95 to 1.9.

Namely at energies higher 100 GeV the new mechanisms of secondary particle generation can appear and change the  $\mu^+/\mu^-$  ratio. The recent calculations [2] show that taking into account the discovered quark-gluon state of matter during generation of secondary particles in  $pA$ -interactions leads to progressive decrease of value of  $k$  from  $\sim 1.3$  for 100 GeV to 1.22 and 1.14 for 1 and 10 TeV, respectively. So the value of  $k$  in the energy range  $> 1$  TeV where the number of available experimental data is quite low is of particular interest.

Nowadays, the LVD data can be used to obtain the

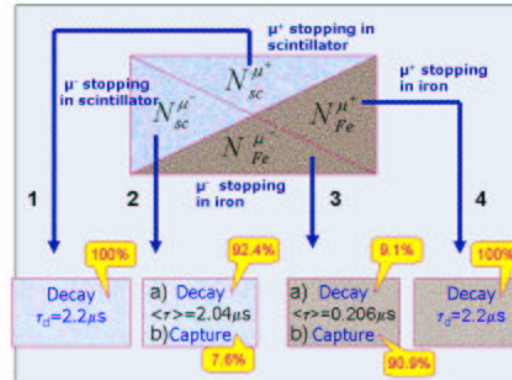


Fig. 1: The stopping muon processes in the LVD materials

positive excess of near-vertical muons of such energies and to evaluate the stopping muons charge composition. The minimal depth of LVD location is 3000 m.w.e. Thus only muons with energy higher than 1.3 TeV at the surface can reach this depth. For stopping muons their average energy at the surface is 1.8 TeV.

## II. DETECTION METHOD

LVD [3] is situated under the Gran Sasso Mountain in central Italy. It is a scintillation-tracking detector with iron-carbohydrate target. The iron mass is about 50% of the total detector mass (2 kt). Scintillator and iron are uniformly distributed in the volume of the apparatus, with a modular structure made of 840 elementary cells. They are grouped in three towers, each consisting of 7 layers. The tower dimension is  $13 \times 6 \times 10$  m<sup>3</sup>. The cell is a scintillation counter with a volume of  $100 \times 100 \times 150$  cm<sup>3</sup> surrounded by iron, whose mean thickness is 2.9 cm. Eight counters are assembled into the iron module. The configuration of iron and scintillator permits to detect the products of nuclear interactions both in scintillator and in iron using the scintillation counters. The detection energy threshold is 5 MeV.

The iron mass is equal to 45% of the total mass in the inner part of the tower. So the ratio of the muon stopping in the scintillator and in iron is  $N_{st}^{sc}/N_{st}^{Fe} = M_{sc}/M_{Fe} = 1.21$ . The  $\mu$  stopping processes in the LVD materials are presented in Fig. 1.

The charge composition  $k$  of the muon flux can be ob-

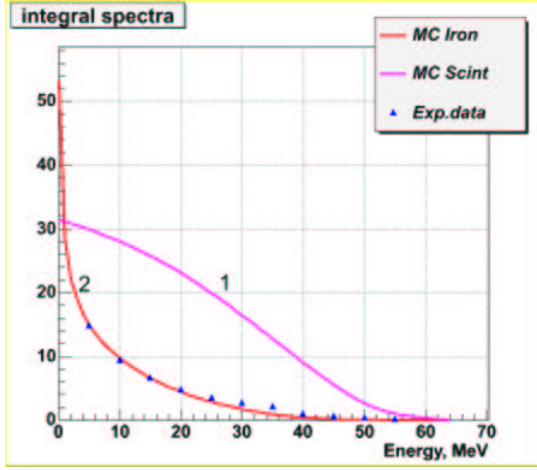


Fig. 2: The integral energy spectra of  $\mu^\pm$ -decay events in scintillator (1) and  $\mu^+$  ones in iron (2). The curve (1) has been normalized by total number of detecting  $\mu^\pm$ -decay events with energy  $>5$  MeV. The curve (2) has been normalized by experimental data of  $\mu^+$ -decay in iron.

tained by measuring the fraction of negative or positive muons in the total number of stopping muons:

$$k = \frac{R^+}{R^-} = \frac{R_{sc}^+}{R_{sc}^- - R_{sc}^+} = \left( \frac{R_{sc}^\pm}{R_{sc}^+} - 1 \right)^{-1} \quad (1)$$

where  $R_{sc}^\pm$  and  $R_{sc}^+$  are the numbers of  $\mu^\pm$  and  $\mu^+$  stopping in a counter, normalized to the muon flux for the counter that is  $R_{sc}^\pm = N_{sc}^\pm/N_\mu$ ,  $R_{sc}^+ = N_{sc}^+/N_\mu$ . The peculiarities of LVD setup such as the configuration of iron and scintillator, the electronic dead time of 1  $\mu s$ , the presence of photomultiplier afterpulses, allow establishing

- a) the number of  $\mu^\pm$  -decays in scintillator  $_d N_{sc}^\pm$  ;
- b) the number of  $\mu^+$  -decays in iron  $_d N_{Fe}^+$  .

The value of a) is determined by looking for pulses in the same scintillation counters crossed by muon, i.e. placed along the muon track. The value of b) can be obtained by using the data of the counters outside the muon track. Using a) we can get the total number of stopping muons in scintillator. From b) we can go to  $_d N_{sc}^+$  so,

$$_d N_{sc}^+ \propto \frac{M_{sc}}{M_{Fe}} \cdot _d N_{Fe}^+ \quad (2)$$

We can detect only  $\mu$  decays but not captures. As follows from Fig. 1 number of  $\mu$  decays in iron is less than number of  $\mu$  stoppings. This fact is taken into account by using detection efficiency.

**Stopping  $\mu^+$  decays only.**

$$\mu^+ \rightarrow e^+ \nu_e \tilde{\nu}_\mu, \tau_d = 2.2 \mu s.$$

The energy spectrum of  $e^+$  has a maximum at  $\sim 37$  MeV and the greatest energy of 52.8 MeV.

The positrons together with gamma-quanta from electromagnetic cascades (if muon decays in iron) and gamma-quanta from electron-positron annihilation are detected

in the scintillation counters. The observed energy spectrum and detection efficiency of  $\mu^+$  decays in scintillator differ radically from the corresponding values of  $\mu^+$  decays in iron (Fig. 2).

**Stopping  $\mu^-$**  in detector materials may either decay or be captured by iron and carbon nuclei.

The energy spectrum of negative muon decay products is the same as for positive one, but the time characteristics depend on nuclear composition of the matter.

The rate  $\Lambda_c$  of  $\mu^- A$  -capture depends on  $Z$  as  $Z^4$ . Thus, in case of stops in iron negative muons are mainly captured by iron nuclei (90.9% of all  $\mu^-$ -stops in iron), and in case of stops in scintillator they mainly decay (92.4% of all  $\mu^-$ -stops in scintillator).  $\mu^-^{12}C$ -captures do not contribute to the final result because of the small fraction of  $\mu^-$ -captures in the scintillator and of the small duration (1 ms) of the time window for the data taking with respect to the average life time of the products of the reaction  $\mu^-^{12}C \rightarrow ^{12}B \nu_\mu, ^{12}B \rightarrow ^{12}C e^- \tilde{\nu}_e$  ( $\tau \sim 39ms$ ). The fraction of detectable muon captures in the scintillator is thus negligible ( $\sim 0.1\%$ ). The probability of  $\mu^-$ -capture by a free proton is 200 times less than the probability of  $\mu^-^{12}C$ -capture, so this process was not taken into account.

$\mu^- Fe$ -capture is accompanied by gamma-quanta emission (0.32 gamma-quanta per capture) with energies of 3 - 10 MeV [4] and also emission of  $\sim 1.13$  neutrons in average [5]. The time distribution of gamma-quantum pulses is described with a  $\mu^-$  life-time in iron:  $\tau_{Fe} = 1/(\Lambda_c^- + \Lambda_d^+) = 0.206 \mu s$  (at  $\Lambda_c^- = 44.0 \cdot 10^5 s^{-1}$ ). The same exponent corresponds to the time distribution of  $\mu^-$  -decays in iron. Although they represent a large fraction of events,  $\mu^- Fe$ -capture are not considered in our analysis because bulk of the events in the 0.25 - 1.00  $\mu s$  time interval is the composition of the processes 3a, 3b, 4 (Fig. 1, Fig. 3). The range 0 - 0.25  $\mu s$  is used to define a counter crossed by muon or placed out the muon track.

### III. THE SELECTION CRITERIA

We analyzed the single muon events in the first LVD tower. A single muon event is defined as the presence of pulses with energy higher than 50 MeV in several counters (from 2 to 11), in time coincidence within 0.25  $\mu s$ . The time 0 corresponds to the first pulse of the cluster of pulses originated by muon. The cluster is the set of muon pulses from counters crossed by a muon. Such a criterion allows to eliminate the local produced muons, multiple muons and muons with accompanying shower.

The pulses with energies 5 - 60 MeV in the counters crossed by a muon in a time window 1 - 10  $\mu s$  are regarded as  $\mu^\pm$ -decay candidates in scintillator. The beginning of the time interval is determined by a counter dead time  $t_d = 1.0 \mu s$  after muon ionization loss pulse (Fig. 3a).

The time accuracy for pulses in muon event is  $\pm 70$  ns, TDC discreteness is 12.5 ns; the counter energy

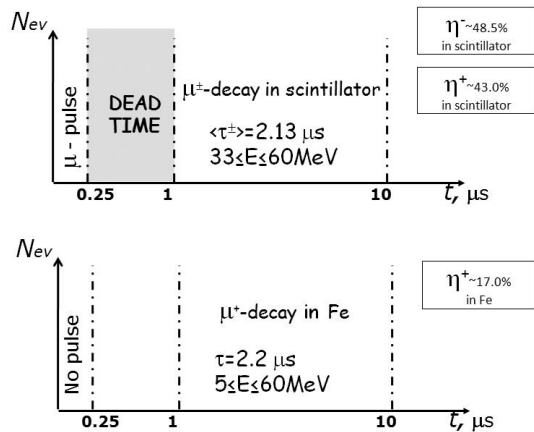


Fig. 3: The  $\mu$  decay events selection time diagrams for of: *up*- decays in scintillator (counters along muon track), *down*- decay in iron (counters out of muon track)

resolution is  $\sim 25\%$  for 5 - 60 MeV energy range.

The pulses in the same energy and time intervals but in counters outside the muon track (that is, without any pulse in the  $0.25 \mu s$  time window) are considered as candidates for  $\mu^+$ -decays in iron. Due to the  $\mu^-$  lifetime in iron, the events of  $\mu^- Fe$ -captures and  $\mu^-$ -decays are situated between 0 and  $1 \mu s$  (Fig. 3b).

The data of 110 counters from 120 inner ones (from 2nd to 6th levels of first tower) were used in the analysis. They were selected according to the time characteristics and stability.

#### IV. BACKGROUND ESTIMATION

The PM afterpulses are the main background for the selection of  $\mu^\pm$ -decays in scintillator and the  $\gamma$ -quanta induced by  $nFe$ -captures are background for  $\mu^+$ -decays in iron. Neutrons are also produced in  $\mu^- Fe$ -captures. To exclude the background due to the PM afterpulses in the 1-10  $\mu s$  window, all muon events were divided into 2 groups: through-going and “quasi-stopping”. The muon was regarded as through-going if it produces a pulse in 0 -  $0.25 \mu s$  time interval with energy higher than 10 MeV in the 1st level counter. The remaining events are regarded as quasi-stopping. Obviously, among quasi-stopping muons the fraction of muons really stopped in the LVD detector is small because some muons can leave the detector through a corridor. Since there is no muon decay, the first group of events allows to determine the afterpulse rate for each counter.

The number of real muon decays is thus given by the difference between number of pulses in the 1 - 10  $\mu s$  window for the quasistopping events and the normalized number for throughgoing muons.

To obtain a time distribution of the decay events in the 1 - 10  $\mu s$  time interval we repeat the procedure, changing the starting time from  $1 \mu s$  to  $10 \mu s$ . Thus we get the integral time distribution and total amount (at  $t = 0$ ) of

$\mu^\pm$ -decays in scintillator. At this stage we use  $\mu^\pm$ -decay exponent  $\tau = 2.2 \mu s$  to eliminate the background from  $nFe$ -captures which is almost flat in the range 1 - 10  $\mu s$ .

#### V. RESULTS

The analysis of muon charge composition is performed using data of the 1st tower during 6 years containing 10986384 muon pulses in 110 counters. We selected 2299  $\mu^\pm$ -decays in scintillator with an energy, released by the decay products, larger than 33 MeV. This additional cut was required to remove the events when muon crosses a counter, then stops and decays in iron wall while the decay products reenter into the same counter. The energy release of the products of muon decay in iron does not exceed 33 MeV which is approximately the mean value of the free muon decay spectrum (Fig 2).

The number of  $\mu^+$ -decays in iron is 1335.

##### A. Number of $\mu^\pm$ -decays in scintillator

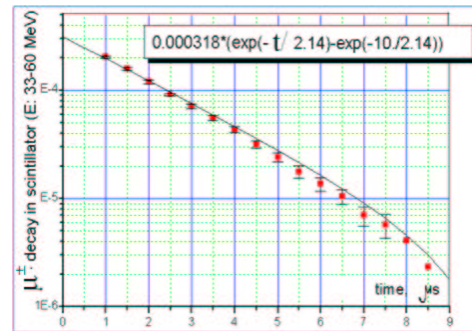


Fig. 4: The integral time distribution for  $\mu^\pm$ -decays in scintillator

We obtain the value of  $R_{sc}^\pm$  in (1) using the experimental number of  $^{exp}R_{sc}^\pm = 3.18 \cdot 10^{-4}$  with energy threshold of 33 MeV and a corresponding efficiency  $\eta_{sc}^\pm$ :

$$R_{sc}^\pm = \frac{^{exp}R_{sc}^\pm}{\eta_{sc}^\pm} \quad (3)$$

$^{exp}R_{sc}^\pm$  is the value of the  $^{exp}R_{sc}^\pm(t)$  function at  $t=0$  Fig 4. Each point in the plot presents the value  $^{exp}R_{sc}^\pm$  averaged over 110 counters at fixed  $t_{fix}$  from the time interval 1- 10  $\mu s$

$$^{exp}R_{sc}^\pm(t_{fix}) = \frac{\sum_{100} (^{exp}R_{sc}^\pm(t_{fix}))}{110}$$

The value of  $\eta_{sc}^\pm$  depends on the detection efficiency (for energy threshold of 33 MeV) of  $\mu^+$ ,  $\mu^-$ -decays, on the charge composition of muons  $c^+ = \frac{k}{k+1}$ ,  $c^- = \frac{1}{k+1}$  and on the fraction  $p_d^-$  of  $\mu^-$ -decays in scintillator:

$$\eta_{sc}^\pm = c^+ \eta_{sc}^+ + c^- \eta_{sc}^- p_d^-, \quad (4)$$

$$\begin{aligned}
p_d^- &= 1 - p_d^-(^{12}C) = \\
&= 1 - \frac{\Lambda_c(^{12}C)}{\Lambda_c(^{12}C) + \Lambda_d(\mu^-)} \\
&= \frac{0.37 \cdot 10^5}{0.37 \cdot 10^5 + 4.52 \cdot 10^5} = 0.924
\end{aligned} \tag{5}$$

$\Lambda_c$ ,  $\Lambda_d$  are the rates of  $\mu^-$ -capture and  $\mu^-$ -decay in scintillator. The values  $\eta_{sc}^+$  and  $\eta_{sc}^-$  were calculated using a GEANT4 Monte Carlo simulation:  $\eta_{sc}^+ = 0.430$ ,  $\eta_{sc}^- = 0.485$ . Thus we get:

$$\eta_{sc}^\pm = 0.43 \frac{k}{k+1} + 0.924 * 0.485 \frac{1}{k+1} \tag{6}$$

To obtain the number of  $^{exp}R_{sc}^\pm$  we fitted the experimental integral distribution in Fig 4. with the exponent  $\tau^\pm = 2.135 \mu s$ . Of course, the exponent depends on both the  $\mu^+$ ,  $\mu^-$  - lifetime in scintillator ( $\tau^+ = 2.2 \mu s$ ,  $\tau_{sc}^- = 2.045 \mu s$  and the muon flux charge composition but the dependence is weak: we have found that a variation of  $k$  from 1.0 to 1.5 changes the exponent  $\tau^\pm$  from 2.13  $\mu s$  to 2.14  $\mu s$ . On the other hand,  $^{exp}R_{sc}^\pm$  varies insignificantly while changing  $\tau^\pm$  value in the range 2.13 - 2.14  $\mu s$ .

### B. Number of $\mu^+$ -decays in iron

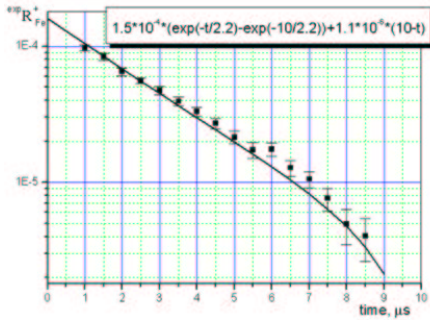


Fig. 5: The integral time distribution for  $\mu^+$  -decays in iron.

We obtain the value of  $R_{Fe}^+$  using the experimental value of  $^{exp}R_{Fe}^+ = 1.5 \cdot 10^{-4}$  (Fig 5) taking into account the mass factor  $M = M_{sc}/M_{Fe} = 1.21$ , the MC efficiency  $\eta_{Fe}^+ = 0.17$  (with the energy threshold of 5 MeV) and estimating the amount  $B = \eta_b^\pm R_{sc}^\pm$  of decaying  $e^\pm$  which penetrate into a counter outside the muon track from a neighbor counter where  $\mu^\pm$  decayed:

$$\begin{aligned}
R_{sc}^+ &= \frac{M}{a\eta_{Fe}^+} (^{exp}R_{Fe}^+ - B) = \\
&= \frac{M}{a\eta_{Fe}^+} (^{exp}R_{Fe}^+ - \frac{\eta_b^\pm}{\eta_{sc}^\pm} \cdot ^{exp}R_{sc}^\pm)
\end{aligned} \tag{7}$$

The constant  $a$  takes into account the fact that a counter detects  $\mu^+$ -decays in iron of a neighbour counter, thus  $a = 2$ . The coefficient  $\eta_b^\pm$  is the fraction of  $\mu^\pm$ -decays in scintillator that produce pulses with energy larger than 5 MeV in a neighbor counter:  $\eta_b^\pm = c^+ \eta_b^+ + c^- \eta_b^- p_d^-$ . The

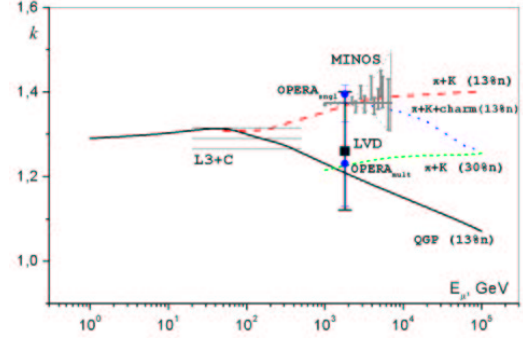


Fig. 6: The measured  $k$  value and the theoretical dependence  $k(E_\mu)$  [2]. The square point is the LVD result, the straight lines the L3+C data [1] in the energy range from 2 to 500 GeV, the bars are the MINOS data [7], the circle is OPERA [8], the curves are the theoretical predictions [2].

values of  $\eta_b^+$  and  $\eta_b^-$  were calculated using GEANT4:  $\eta_b^+ = 0.06$ ,  $\eta_b^- = 0.04$ .

So, the ratio of  $R_{sc}^\pm/R_{sc}^+$  in (1) is

$$\frac{R_{sc}^\pm}{R_{sc}^+} = \left( \frac{M\eta_{sc}^\pm}{2\eta_{Fe}^\pm} \cdot \left( \frac{^{exp}R_{Fe}^+}{^{exp}R_{sc}^\pm} - \frac{\eta_b^\pm}{\eta_{sc}^\pm} \right) \right)^{-1} \tag{8}$$

and

$$k = \left\{ \left( \frac{M\eta_{sc}^\pm}{2\eta_{Fe}^\pm} \left( \frac{^{exp}R_{Fe}^+}{^{exp}R_{sc}^\pm} - \frac{\eta_b^\pm}{\eta_{sc}^\pm} \right) \right)^{-1} - 1 \right\}^{-1} \tag{9}$$

The right part of the equation also depends on  $k$ . Thus we solve it numerically (segment dichotomy).

In conclusion, we have determined the charge ratio for the flux of near-to-vertical muons in energy range from  $\sim 1$  TeV to  $\sim 3$  TeV at sea level and with average energy about 1.8 TeV:

$$k = 1.26 \pm 0.11 \pm 0.04. \tag{10}$$

The first error is systematic while the second value is statistic. The systematic error depends mainly on experimental values  $^{exp}R_{sc}^\pm$ ,  $^{exp}R_{Fe}^+$  and calculated numbers of  $\eta_{Fe}$ ,  $\eta_{sc}$ ,  $\eta_b$ .

The value of  $k$  in comparison with the theoretical prediction is shown in Fig 6.

## VI. ACKNOWLEDGMENT

This work is made with the RFFI financial support (grants 09-02-00300a, SSchool-959.2008.2) and Program for Fundamental Research of Presidium of RAS "Neutrino Physics".

## REFERENCES

- [1] The L3 Collaboration, *arxiv:hep-ex/0408114 v1 23 Aug 2004*
- [2] L.V. Volkova *Phys. of Atomic Nuclei (2008)*, 71, 1782
- [3] LVD Collaboration, *Proc of 27 ICRC*, 3 (2001), 1093-1095
- [4] Veisenberg A.O. *Mu-meson*, Nauka, Moscow (1964)
- [5] McDonald B. *et al.*, *Phys. Rev.*, 139 (1965), 1253
- [6] Dadykin V.L. *et al.*, *17th ICRC, Paris, 1981 p. 187-190*
- [7] Mufson S.L. and Rebel B.J. for the MINOS collaboration, *30th ICRC, Mexico, 2007*
- [8] M. Sioli for the OPERA collaboration, *in ICRC09, (these proceedings), 2009*